CityZen

megaCITY - Zoom for the Environment

Collaborative Project

7th Framework Programme for Research and Technological Development

Cooperation, Theme 6:

Environment (including Climate Change)

Grant Agreement No.: 212095

Deliverable D1.1.4, type R

Analysis of the evolution of air pollution in the studied high emissions areas over the 10 past years

Due date of deliverable: project month 34

Actual submission date: project month 35

Start date of project: 1 September 2008 Duration: 36 months

Name of lead beneficiary for this deliverable: IUP-UB

Scientist(s) responsible for this deliverable: Andreas Richter, Andreas Hilboll, Folkard Wittrock, Mihalis Vrekoussis

Project co-funded by the European Commission within the Seventh Framework Programme (2007-2013)		
Dissemination Level		
RE	Restricted to a group specified by the consortium (including the Commission Services)	X

Analysis of the evolution of air pollution in the studied high emissions areas over the 10 past years

1 Global trends in NO_2

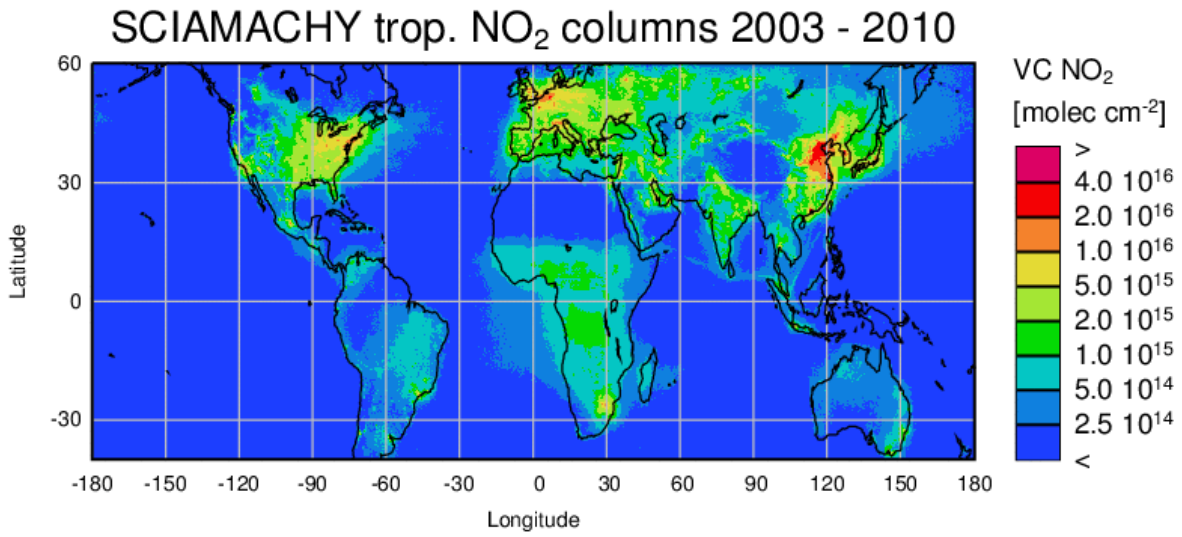

Figure 1: Long-term average of SCIAMACHY tropospheric NO_2 columns. Pollution hot-spots over industrialised countries are evident as well as regions affected by biomass burning. From the Red Sea towards China and Japan, a thin line of ship emission NO_2 is also present. The colour scale is logarithmic to capture the 2 orders of magnitude spread in NO_2 values from the shipping lanes to the most polluted areas in China.

Nitrogen oxides (NOx = NO + NO_2) are key pollutants in the troposphere. They determine ozone levels both in the background atmosphere and, together with VOCs, in polluted environments. They are also involved in the formation of acid rain and in eutrophication of water bodies with large consequences for the biosphere. The main sources of nitrogen oxides are anthropogenic, predominantly from the combustion of fossil fuels. Natural sources include biomass burning and soil emissions which both in part are also related to human activities and lightning.

The sources of NOx are reflected in the global distribution of nitrogen dioxide (NO_2) columns measured from space. Using the Differential Optical Absorption Spectroscopy (DOAS) method, global NO_2-maps can be retrieved from spectrally resolved observations of the backscattered solar radiation by instruments such as GOME, SCIAMACHY, OMI, or GOME-2. An example is shown in Figure 1 highlighting the large range of NO_2 values found from the remote ocean to the most polluted places. As the tropospheric lifetime of NO_2 is of the order of hours to days and most NOx sources are on the ground, the NO_2 column distribution is closely linked to NO_2 concentrations in the boundary layer. At the same time, NO_2 columns are also directly linked to NOx emissions, albeit with factors depending on lifetime and thus season and location (*e.g. Martin et al., 2002).*

The first global tropospheric NO_2 observations became possible with the GOME instrument in late 1995, and the long-term data set established since then enables analysis of changes in NO_2 columns and thereby pollution levels and NOx emissions. Use of data from multiple sensors requires careful treatment of differences between instruments and this will be discussed in more detail in section 3.

However, data from the SCIAMACHY instrument alone already span more than 8 years, and as a first approach, changes in this data set will be investigated.

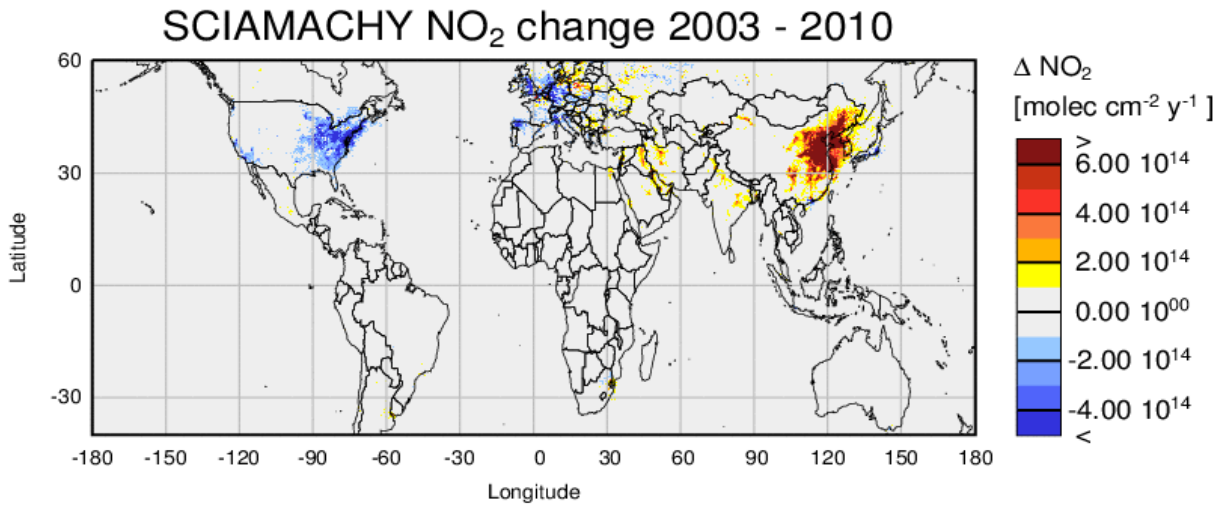

Figure 2: Mean annual change of tropospheric NO_2 derived from SCIAMACHY measurements in the time period 2003 – 2010. Red colours indicate increasing NO_2, blue colours decreasing trends.

Following the approach presented in *Richter et al., 200*5, SCIAMACHY data from 2003 to 2010 have been analysed and annual means have been produced. In the retrieval, the a priori used was kept constant to avoid that model predicted changes impact on the trend analysis. Using the 8 annual means, a linear trend was fitted for each 0.125° x 0.125° grid cell and the slope of the fit plotted in Figure 2. No attempt was made to select data for statistical significance but this was done in the more detailed analysis reported below. Similar trend studies have also been reported in *van der A 2006* and *2008* and *Stavrakou et al., 2008*.

In Figure 2, a number of interesting observations can be made. First of all, there is a large and very systematic decrease in NO_2 levels throughout the US. With the exception of a few grid boxes, this includes the full area while NO_2 levels in both Mexico and Canada show upward trends. This downward trend over the US is the result of changes in environmental laws as for example for power plants (*Kim et al., 2006, 2009*) but also from general reductions in car emissions. A significant fraction of the large reductions are from the last years, as illustrated in Figure 3 for Los Angeles. This is in agreement with results presented in *Russell et al., 2010*.

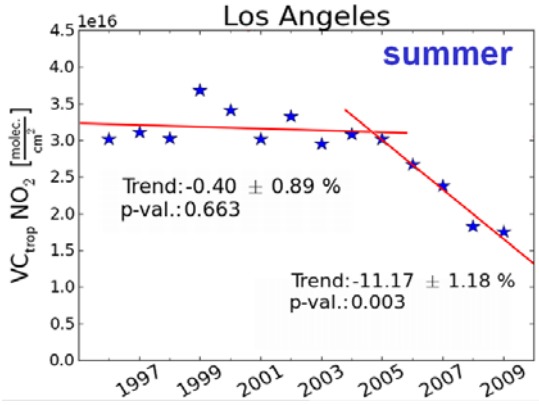

Figure 3: Tropospheric NO_2 evolution in Los Angeles as derived from GOME and SCIAMACHY observations. Only summer values were used. Two separate trends were calculated, one from 1997 – 2005 and one from 2005 – 2009.

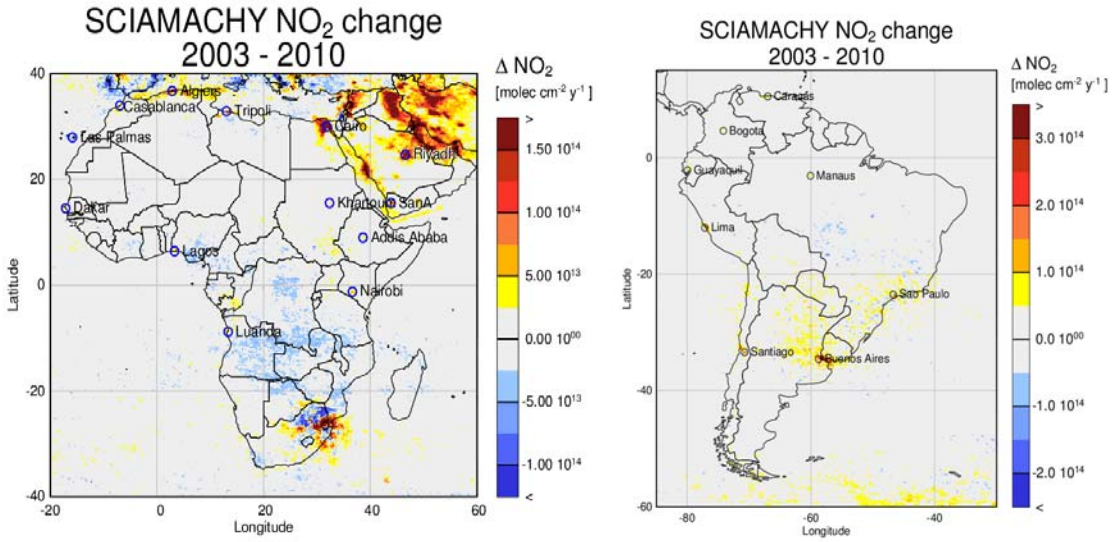

Figure 4. Zoom of Figure 2 for Africa (left) and South America (right). Please note the different colour scales used.

Over Europe, reductions are also evident, but mostly in the Western parts and not as clear as in the US. This is somewhat of a change as compared to the results in *Richter et al., 2005* which found a clear downward trend in the period 1996 – 2002. Systematic reductions in NO_2 are also observed over Japan as from 1996 – 2002.

A very large increase in NO_2 columns is found in China as result of the continuing rapid development of industry and economy in the country with its more than 1 billion inhabitants. A closer look at China will be taken in section 2. At the same time, increasing NO_2 levels are also seen in Arabia, Iran, and India.

As result of the much better spatial resolution of the SCIAMACHY measurements as compared to the GOME data set, changes on the level of individual cities can also be investigated.

In Figure 4, zoomed maps are shown for SCIAMACHY derived NO_2 changes over Africa and South America. As can be seen from Figure 1, the overall NO_2 levels on both continents are much lower than in Europe or Asia. However, when using a different scale, a large number of cities can be identified with an increase of NO_2, including Nairobi, Luanda, Lagos, Tripoli, and Dakar in Africa, and Buenos Aires, Lima, Sao Paulo, Manaus, Santiago de Chile, and Bogotá in South America. This illustrates that on these two continents, changes in air quality are really confined to the large cities, whereas in Europe, the US, and China, very large areas are affected.

As mentioned before, NO_2 levels in Arabian countries have been increasing significantly, indicating economic and population growth. In contrast, NO_2 over Israel has decreased, probably as result of tightening of environmental laws. In the Red Sea and the Gulf of Aden, an increase in ship emitted NO_2 is also visible. Decreases in NO_2 over Central Africa are linked to inter-annual variability in biomass burning and are not considered to be significant. The increased noise in the southern part of Brazil and northern Argentina is linked to increased instrument noise in the Southern Atlantic Anomaly region.

2 Zoom in over China

2.1 Changes in NO_2 over China

Arguably the most dramatic changes worldwide are observed over China. This was already reported for NO_2 in a number of publications (*e.g. Richter et al., 2005, van der A et al., 2006, He et al., 2007, Zhang et al., 2007*). In recent years, economic growth has continued, but aggressive measures have been taken by the Chinese government to limit emissions of pollutants. As can be seen in Figure 5, the increase in tropospheric NO_2 in the Eastern Central part of China (30 – 40°N, 110 – 123°E) has continued with a slowdown in 2008 / 2009, probably as a result of the measures taken for the Olympic Games in Beijing and the following global economic downturn. No indication is seen for an end to this trend and the largest NO_2 columns ever observed are from January 2011 (not shown).

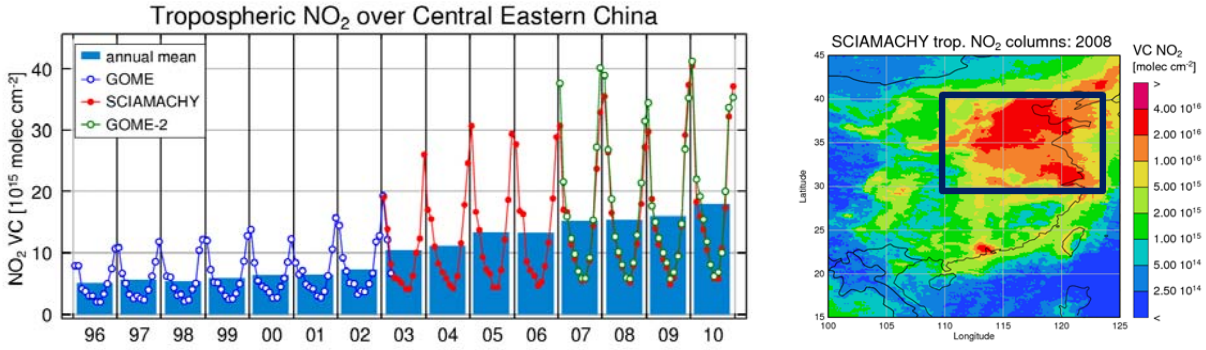

Figure 5: Left: Evolution of tropospheric NO_2 columns above Central Eastern China. Shown are both the monthly averages (dots) and annual means (bars) for GOME and SCIAMACHY. GOME-2 data are also shown as monthly averages in green. Right: Spatial distribution of NO_2 in 2008. The black box indicates the area used for the left figure.

As one would expect, the trend in China is not uniform and both increases in total NO_2 and expansion of high pollution levels to previously cleaner areas are observed. Interestingly, downward trends in NO_2 levels can be seen in the data not only for Taiwan but also for Hong Kong and surrounding areas. This is an indication for changes in emission patterns as emissions from different sectors change and also economic development changes the industrial structure within China.

2.2 Changes in SO_2 over China

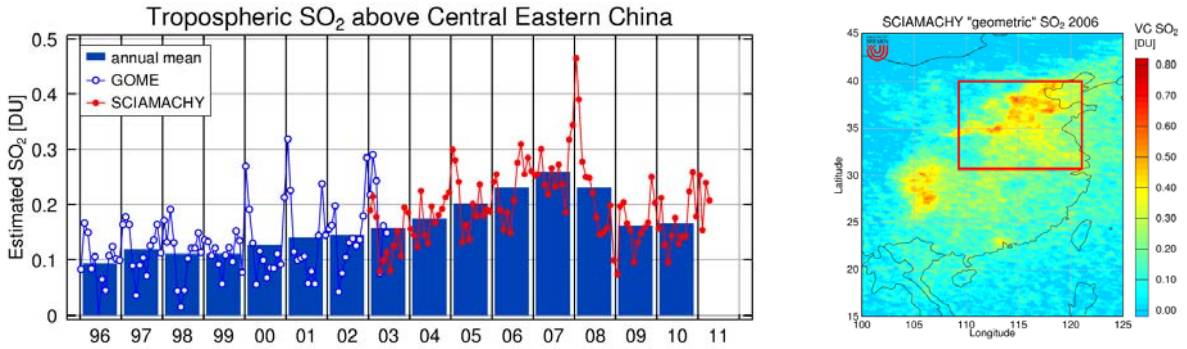

Figure 6: Left: Time evolution of the tropospheric SO_2 burden above Central Eastern China. Bars are annual averages, points are monthly values. The map on the right shows the spatial distribution of SO_2 in 2006, the red box indicating the area used for the left plot.

In addition to NO_2, Sulphur Dioxide (SO_2) columns can also be retrieved from GOME and SCIAMACHY measurements. As the retrieval is performed in the UV, where intensity is smaller and atmospheric scattering is more relevant, it is difficult to derive quantitative numbers without detailed knowledge about aerosol and SO_2 vertical profiles. However, the temporal evolution of the SO_2 burden can be evaluated by using a data set with constant assumptions (in this case a stratospheric airmass factor) and looking at the change in SO_2 over time. This is illustrated in Figure 6 for the same area as used for NO_2. In spite of the large scatter of values, a strong increase in SO_2 levels can be seen until 2007 when flue gas desulphurisation became mandatory for power plants in China, leading to a clear decrease until 2009. However, in the last year of the time series, there is no further decrease but rather indication for a renewed upward trend. This is probably explained by the growing importance of other, not yet regulated sources of SO_2, such as industry and transportation.

It should be pointed out that the observed changes in SO_2 levels have a direct impact on aerosol composition in China, and reduction in the sulphur content will reduce aerosols overall, and reflective aerosols in particular. This is relevant for both visibility and local climate forcing.

2.3 Changes in glyoxal over China

It is expected that not only NO_2 and SO_2 but also VOC-emissions are rising in China. Two VOCs can be measured by satellite, HCHO and glyoxal (*Wittrock et al., 2006, Vrekoussis et al., 2009, 2010*). In contrast to NO_2 and SO_2, anthropogenic emissions of VOCs are small compared to biogenic sources, complicating trend estimates. Also, biomass burning contributes significantly to glyoxal levels, and changes in agricultural practices in China have altered the spatial pattern and intensity of fires related to farming.

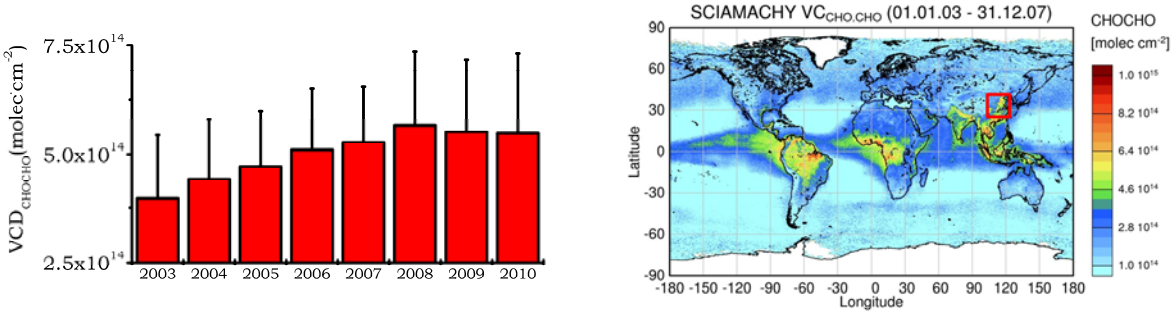

Figure 7: Left: Temporal evolution of glyoxal over Central Eastern China as observed from SCIAMACHY. Right: Global distribution of glyoxal.

In Figure 7, the spatial distribution of glyoxal is shown as derived from SCIAMACHY measurements. As can be seen, the largest values are observed over tropical rain forests, but enhanced columns are also observed in East Asia. In the left panel, the temporal evolution of glyoxal over Central Eastern China is presented. A clear upward trend is found from 2003 to 2008, with a slight reduction in 2009 and no change in 2010. While the relative change is less pronounced than for NO_2, it should be noted that there probably is a significant natural background. Therefore, the relative change of the anthropogenic contribution presumably is much larger. Whether this change is from changes in anthropogenic VOC emissions or in biomass burning practices cannot be decided at this point. Upward trends of HCHO over China have been reported by *De Smedt et al., 2008*, but were considered to be artefacts.

3 Zoom in over MegaCities

As already mentioned in section 1, combination of time series from different instruments needs additional steps which will in the following be described for a combined time series of GOME and SCIAMACHY data.

3.1 Description of trend calculations

3.1.1 Correcting for ground pixel size

The GOME and SCIAMACHY measurements have very different ground pixel sizes: while a GOME ground pixel measures 320km in cross-track and 40km in along-track direction, SCIAMACHY ground pixels have a considerably smaller footprint of 60km by 30km. For homogeneous regions, this leads to negligible differences, but in the case of localized sources, such as megacities, these different ground pixel sizes produce considerable differences (see Figure 8 for an explanation).

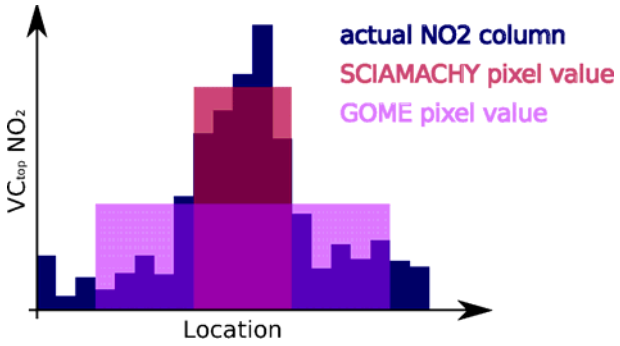

Figure 8: Influence of ground pixel size on retrieved NO_2 columns. Especially when measuring over locally confined NO_2 sources, such as megacities, the pixel size has considerable impact on the measurements. The retrieved NO_2 columns are spatially integrated over the ground pixel, which leads to lower values for ground pixels containing source and background regions.

This effect can easily be seen when comparing maps of monthly mean vertical NO_2 columns from GOME and SCIAMACHY (see Figure 9). The signatures of all major urban agglomerations (like, e.g., Paris, Frankfurt, BeNeLux, Milano, Madrid, Barcelona, Moscow, Cairo, …) can be seen as clear spots in the SCIAMACHY measurements, while with GOME, these enhanced values are systematically blurred in the direction of the instrument's swath.

3.1.2 Calculation of correction factors for gridded GOME data

In order to overcome these instrumental differences and create one joint dataset of tropospheric NO_2 measurements spanning the years 1996-2010, a database of correction factors to be applied to gridded GOME measurements was calculated. For this purpose, use is being made of SCIAMACHY's backscan measurements (see Figure 10), which have a ground pixel size of 240km by 30km, which is reasonably close to GOME's ground pixel resolution of 320km by 40km. The correction factors are calculated on a 0.125° x 0.125° grid by dividing SCIAMACHY's forward by backscan measurements. Compared to purely mathematical blurring techniques (i.e. Gaussian blurring), this method has the advantage of being based on the actual measurements. In this study, a monthly climatology of correction factors was calculated from SCIAMACHY measurements from January 2003 to December 2009. Using these factors, a dataset of corrected daily GOME measurements was calcu-

lated by multiplying the gridded GOME measurements with the correction factor climatology for the appropriate month (see, e.g., Figure 11).

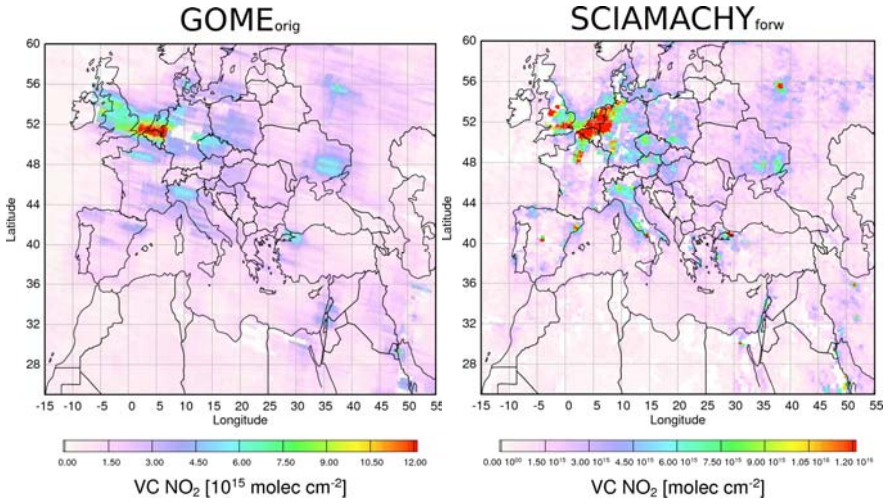

Figure 9: Vertical NO_2 columns from GOME (left) and SCIAMACHY forward scan (right) for May 2003.

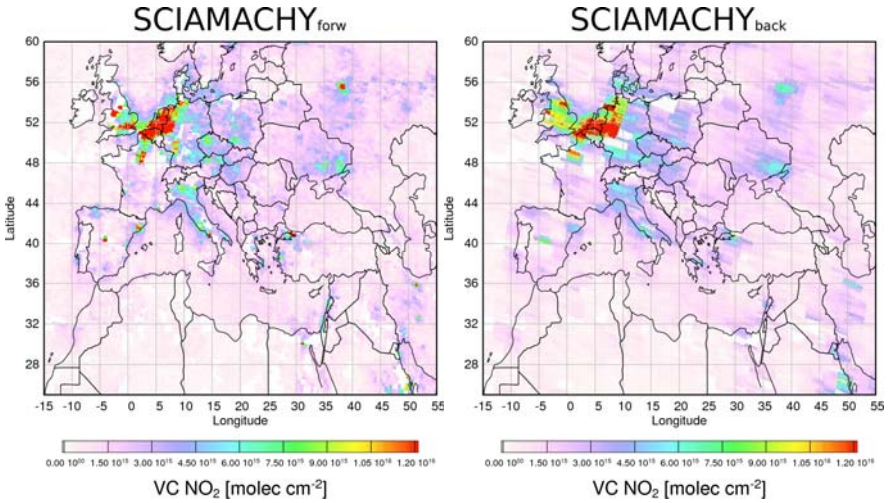

Figure 10: Tropospheric NO_2 columns for May 2003 using only the forward scans (left) and only the backward scans (right).

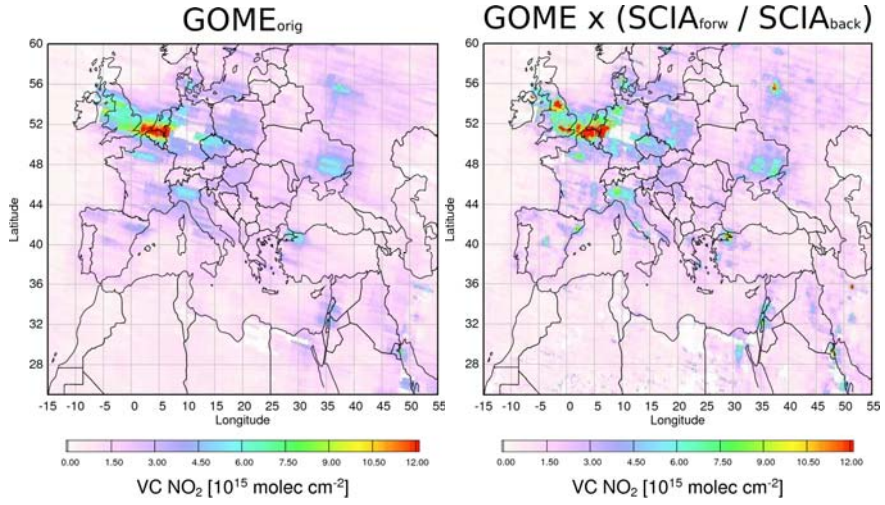

Figure 11: GOME tropospheric NO_2 for May 2003 before (left) and after (right) application of the resolution correction.

3.1.3 Evaluation of the corrected GOME dataset

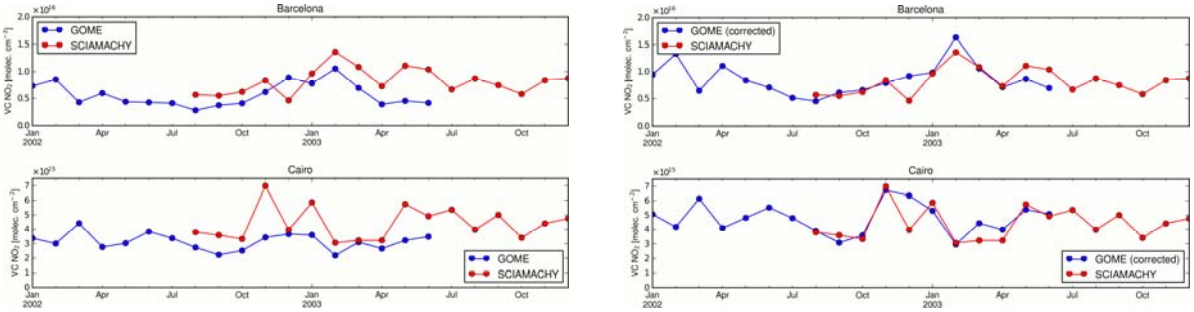

Figure 12: Time-series of tropospheric NO_2 columns over Barcelona and Cairo. Left: original data, right: pixel-size-corrected GOME and original SCIAMACHY measurements

When comparing Figure 9 and Figure 11, it becomes apparent that the spatial structures of corrected GOME measurements and SCIAMACHY measurements are quite similar. These similarities become even more apparent when comparing the months for which both GOME and SCIAMACHY measurements exist (Aug. 2002 – June 2003). While GOME measurements are, as expected, lower than SCIAMACHY measurements by about 10% - 20%, the time-series of tropospheric NO_2 columns over individual urban agglomerations show an almost perfect match when comparing the corrected GOME dataset with SCIAMACHY measurements (see Figure 12).

3.1.4 Constructing the underlying dataset

GOME and SCIAMACHY measurements were evaluated using the DOAS method, a stratospheric correction and airmass factors as described in D1.1.1 and D1.1.5. All data are then gridded on a daily global 0.125x0.125° grid. From these gridded daily values, monthly averages are calculated, yielding a dataset of monthly global gridded vertical tropospheric NO_2 columns from April 1996 until December 2010, where for the months August 2002 until June 2003, there are two values (one for corrected GOME, one for SCIAMACHY). For the resulting consistent dataset, GOME data have been employed until December 2002, and SCIAMACHY data have been used from January 2003 onwards.

3.1.5 Defining city regions of interest

When one is interested in investigating the temporal evolution of tropospheric pollution for small localized regions, such as cities, one big challenge is to find appropriate definitions of the areas of interest. When choosing too small a region, the effects of changing city spread will be ignored. On the other hand, when the regions are chosen big enough to account for city growth, it will be hard to attribute the resulting changes in NO_2 columns to either city growth or actual changes of NO_2 concentration within the city center.

In this study, the quantity of interest is the NO_2 pollution of urban agglomerations as a whole. Therefore, the areas investigated have been chosen to be large enough to accommodate for the growth of the city within the time period of the study. The tropospheric NO_2 columns themselves (their maximum over the 1996-2010 period, to be precise) have been used to define city areas by eyesight, selecting rectangular areas (in the latitude/longitude grid) encircling the sharp gradient dividing city and background areas.

3.2 Results

Using the corrected and merged dataset, trend analysis was performed for the CityZen regions and some additional areas of interest. As early results indicated that results depend on season, separate analysis was performed on annual, summer, and winter data. The results are shown in Figure 13 and summarised in Table 1.

A number of different observations can be made on the trends.

First of all, winter values are higher and more variable in all regions with maybe the exception of Cairo. Therefore, trends in winter are expected to be less reliable. For Bucharest, the seasonality is larger in SCIAMACHY than in GOME data. This could be indication for some remaining resolution related differences between the two data sets.

In the Po valley region, results for all seasons and both areas indicate a consistent downward trend in NO_2, as expected from emissions reductions. The same situation is found in the BeNeLux region with slightly larger variability in the results. These two results are robust and underline the downward trend in pollution which is also apparent in the SCIAMACHY data set alone (Figure 2).

In Cairo, a clear upward trend is observed, which is smaller in summer than in winter. Winter values show larger scatter, but the overall upward trend is very consistent from year to year. Again, this is in excellent agreement with the SCIAMACHY only change shown in Figure 2.

Region	Annual trend [% / yr]	Summer trend [% / yr]	Winter trend [% / yr]
Athens	–	–	–
BeNeLux (small)	–	-1.2	–
BeNeLux (big)	-1.7	-1.5	-0.9
Cairo	+6.1	+3.3	+7.7
Eastern Mediterranean	–	-0.4	+1.7
Istanbul	+2.5	+1.3	+6.1
Po Valley (small)	-1.9	-1.4	–
Po Valley (big)	-1.8	-1.4	-1.4
Bucharest	+3.1	+1.1	+4.8
London	–	-1.8	+2.4
Rome	–	-1.0	+1.9

Table 1: Annual linear growth rates of vertical tropospheric columns NO_2 from the combined GOME/SCIAMACHY dataset (Apr. 1996 – Dec. 2010), for selected European urban agglomerations. Only significant trends are shown ($p \leq 0.05$). For the annual trends, the average of all monthly averages of a year have been calculated (starting with 1997); for the seasonal trends, the averages of the three months June, July, August (summer) and December, January, February (winter). Linear regression has been performed on each of the time-series individually. The trends have been calculated as the slopes of the regression line, relative to the 1998 value for the annual trends, and relative to the season's 1996 value for the seasonal trends.

The situation in London is less clear, with a downward trend in summer and an upward trend in winter. Visual inspection of Figure 13 shows that again winter values are more scattered and the trend possibly dominated by individual outliers while the summer trend appears to be more robust.

Finally, evolution of NO_2 in the Eastern Mediterranean is heterogeneous and no clear linear pattern can be discerned. As for the other regions, winter values show more variability with much enhanced columns in some years.

Differences between summer and winter trends could have several reasons. One difference is the longer lifetime of NO_2 in winter, which makes transport more of a problem for the trend analysis. Also, depending on meteorological conditions, accumulation of pollutants over several days could lead to large enhancements of NO_2 which are not caused by increases in NOx emissions. As a result of the larger solar zenith angle, measurements in winter also have larger uncertainties, at least in middle and high latitudes. All these reasons lend more confidence to the summer trends. On the other hand, there could also be real differences in the trends in summer in winter, for example if summer trends were determined mainly by reductions in strongly regulated vehicular emissions, while winter values could be driven by heating.

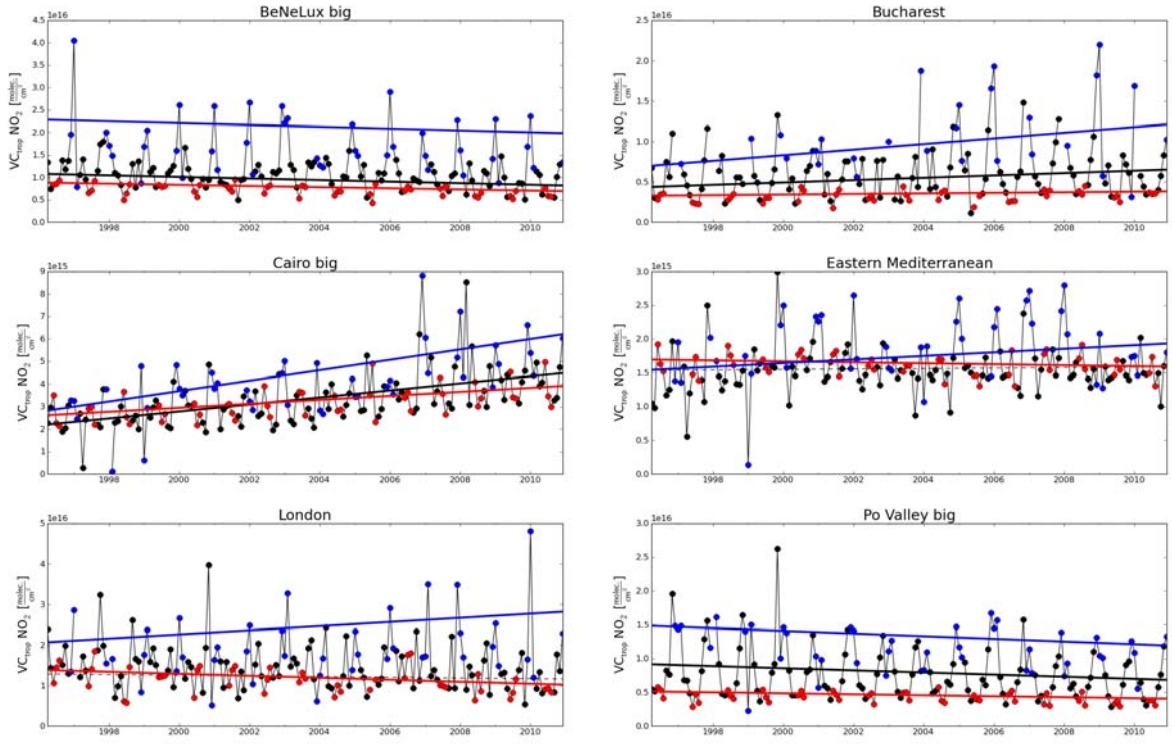

Figure 13: Time-series of monthly mean vertical tropospheric NO_2 columns over selected European urban agglomerations. Summer months (JJA), winter months (DJF), and remaining months are depicted by red, blue, and black dots, respectively. Significant linear trends of summer, winter, and annual means are shown using red, blue, and black solid thick lines, respectively. Non-significant linear fit results are shown as thin dashed lines.

4 Summary

Measurements from the GOME and SCIAMACHY instruments have been analysed for NO_2, SO_2, and glyoxal in the time period 1996 – 2010. Large changes were found for NO_2 in many regions of the world, most notably a strong decrease over the US, a moderate decrease over Europe, and a large upward trend over China and many large cities in both developing and the newly industrialising countries.

In China, large increases in NO_2 are observed throughout the time period, with a levelling off in 2008 / 2009 during the Olympics and the subsequent economic downturn, but increasing values in 2010. For SO_2, a large increase until 2007 was followed by a steep decrease, as flue gas desulphurisation was implemented in power plants, but the decline has stopped in 2010. Levels in glyoxal increased until 2008 but were lower in 2009, possibly also related to reductions in anthropogenic emissions.

Detailed trend analysis of the combined GOME-SCIAMACHY NO_2 data set requires correction for the change in spatial resolution between the two instruments, and a novel algorithm was developed to achieve this. The merged data set gives evidence for significant downward trends of NO2 in the BeNeLux area and the Po valley region, less clear reductions for London, large increases in the Cairo area and ambiguous results for the Eastern Mediterranean. Trends for summer and winter months often differ and this should be investigated in more detail in the future.

5 References

Boersma, K.F., H.J. Eskes and E.J. Brinksma, Error Analysis for Tropospheric NO_2 Retrieval from Space, *J. Geophys. Res.* **109** D04311, doi:10.1029/2003JD003962, 2004

De Smedt, I., Müller, J.-F., Stavrakou, T., van der A, R., Eskes, H., and Van Roozendael, M.: Twelve years of global observations of formaldehyde in the troposphere using GOME and SCIAMACHY sensors, Atmos. Chem. Phys., 8, 4947-4963, doi:10.5194/acp-8-4947-2008, 2008

Franke, K., Richter, A., Bovensmann, H., Eyring, V., Jöckel, P., and J. P. Burrows, Ship emitted NO2 in the Indian Ocean: comparison of model results with satellite data, Atmos. Chem. Phys., **9**, 7289-7301, 2009

He, Y, Uno, I., Wang, Z., Ohara, T., Sugimoto, N., Shimizu, A., Richter, A., Burrows, J. P., Variations of the increasing trend of tropospheric NO2 over central east China during the past decade, Atmospheric Environment, 41, 4865–4876, 2007

Kanakidou M., Mihalopoulos N., Kindap T., Im U., Vrekoussis M., Gerasopoulos E., Dermitzaki E., Unal A., Kocak M., Markakis K., Melas D., Kouvarakis G., Youssef A.F., Richter A., Hatzianastassiou N., Hilboll A., Ebojie F., von Savigny C., Ladstaetter-Weissenmayer A., Burrows J., Moubasher H., Megacities as hot spots of air pollution in the East Mediterranean, Atmospheric Environment, doi:10.1016/j.atmosenv.2010.11.048, 2010

Kim, S.-W., A. Heckel, S. A. McKeen, G. J. Frost, E.-Y. Hsie, M. K. Trainer, A. Richter, J. P. Burrows, S. E. Peckham, and G. A. Grell, Satellite observed U.S. power plant NOx emission reductions and their impact on air quality, Geophys. Res. Lett., 33, L22812, doi:10.1029/2006GL027749, 2006

Kim, S.-W., A. Heckel, G. J. Frost, A. Richter, J. Gleason, J. P. Burrows, S. McKeen, E.-Y. Hsie, C. Granier, and M. Trainer, NO2 columns in the western United States observed from space and simulated by a regional chemistry model and their implications for NOx emissions, J. Geophys. Res., 114, D11301, doi:10.1029/2008JD011343, 2009

Konovalov, I. B., M. Beekmann, R. Vautard, J. P. Burrows, A. Richter, H. Nüß, N. Elansky , Comparison and evaluation of modelled and GOME measurement derived tropospheric NO_2 columns over Western and Eastern Europe, *Atmos. Chem. Phys*., **5**, 169-190, 2005

Konovalov, I. B., Beekmann, M., Richter, A., Burrows, J. P., Inverse modelling of the spatial distribution of NO_x emissions on a continental scale using satellite data, *Atmos. Chem. Phys.*, **6**, 1747-1770, 2006

Konovalov, I., Beekmann, M., Burrows, J. P. , Richter, A., Satellite measurement based estimates of decadal changes in European nitrogen oxides emissions, *Atmos. Chem. Phys.*, **8**, 2623-2641, 2008

Konovalov, I. B., Beekmann, M., Richter, A., Burrows, J. P., and Hilboll, A.: Multi-annual changes of NOx emissions in megacity regions: nonlinear trend analysis of satellite measurement based estimates, *Atmos. Chem. Phys.*, **10**, 8481-8498, doi:10.5194/acp-10-8481-2010, 2010

Martin, R. V., K. Chance, D. J. Jacob, T. P. Kurosu, R. J. D. Spurr, E. Bucsela, J. F. Gleason, P. I. Palmer, I. Bey, A. M. Fiore, Q. Li, R. M. Yantosca and R. B. Koelemeijer, An improved retrieval of tropospheric nitrogen dioxide from GOME, J. Geophys. Res, 107, 4437-4456, 2002.

Richter, A. and J.P. Burrows, Retrieval of Tropospheric NO2 from GOME Measurements, Adv. Space Res., 29(11),1673-1683, 2002

Richter, A., V. Eyring, J. P. Burrows, H. Bovensmann, A. Lauer, B. Sierk, and P. J. Crutzen, Satellite Measurements of NO_2 from International Shipping Emissions, *Geophys. Res. Lett.*, **31**, L23110, doi:10.1029/2004GL020822, 2004

Richter, A., Burrows, J. P., Nüß, H., Granier, C, Niemeier, U., Increase in tropospheric nitrogen dioxide over China observed from space, *Nature*, **437**, 129-132, doi: 10.1038/nature04092, 2005

Richter, A., Begoin, M., Hilboll, A., and Burrows, J. P.: An improved NO_2 retrieval for the GOME-2 satellite instrument, *Atmos. Meas. Tech.*, **4**, 1147-1159, doi:10.5194/amt-4-1147-2011, 2011

Russell, A. R., Valin, L. C., Buscela, E. J., Wenig, M. O., and Cohen, R. C.: Space-basedconstraints on spatial and temporal patterns in NOx emissions in California, 2005–2008,Environ. Sci. Technol., 44, 3607–3615, 2010.

Stavrakou, T., J.-F. Müller, K. F. Boersma, I. De Smedt, and R. J. van der A, Assessing the distribution and growth rates of NOx-emission sources by inverting a 10-year record of NO2 satellite columns, Geophys. Res. Lett., 35, L10801, 2008, doi:10.1029/ 2008GL033521.

Uno, I., He, Y., Ohara, T., Yamaji, K., Kurokawa, J.-I., Katayama, M., Wang, Z., Noguchi, K., Hayashida, S., Richter, A., Burrows, J. P., Systematic analysis of interannual and seasonal variations of model-simulated tropospheric NO2 in Asia and comparison with GOME-satellite data, Atmos. Chem. Phys., 7, 1671-1681, 2007

van der A, R. J., D. H. M. U. Peters, H. Eskes, K. F. Boersma, M. Van Roozendael, I. De Smedt, and H. M. Kelder, Detection of the trend and seasonal variation in tropospheric NO_2 over China, J. Geophys. Res., 111, D12317, doi:10.1029/2005JD006594, 2006

van der A, R. J., H. J. Eskes, K. F. Boersma, T. P. C. van Noije, M. Van Roozendael, I. De Smedt, D. H. M. U. Peters, and E. W. Meijer Trends, seasonal variability and dominant NOx source derived from a ten year record of NO_2 measured from space, J. Geophys. Res., 113, D04302, doi:10.1029/2007JD009021, 2008

Vrekoussis, M., Wittrock, F. , Richter, A. , and P. J. Burrows, Temporal and spatial variability of glyoxal as observed from space, Atmos. Chem. Phys., 9, 4485-4504, 2009

Vrekoussis, M., Wittrock, F., Richter, A., and Burrows, J. P.: GOME-2 observations of oxygenated VOCs: what can we learn from the ratio glyoxal to formaldehyde on a global scale?, *Atmos. Chem. Phys.*, **10**, 10145-10160, doi:10.5194/acp-10-10145-2010, 2010

Wittrock, F., A. Richter, H. Oetjen, J. P. Burrows, M. Kanakidou, S. Myriokefalitakis, R. Volkamer, S. Beirle, U. Platt, and T. Wagner, Simultaneous global observations of glyoxal and formaldehyde from space, Geophys. Res. Lett., 33, L16804, doi:10.1029/2006GL026310, 2006

Zhang, Q. , Streets, D. G., He,K.,Wang, Y., Richter, A., Burrows, J. P., Uno, I., Jang, C. J., Chen, D., Yao, Z., Lei, Y., NOx emission trends for China, 1995–2004: The view from the ground and the view from space, J. Geophys. Res., 112, D22306, doi:10.1029/2007JD008684., 2007